# Supplementary Data

# Supplementary Materials and Methods

## Antibody

Rabbit polyclonal antibody LN1436 was raised against synthetic peptide corresponding to residues 427-461 (HDIENVLLKPENLYN) at the extreme C-terminus of human CLR protein (Accession numbers AAC41994 and AAA62158) and characterized (1).

## Cell Culture

Renal cancer cell lines A498; Caki-1; SKRC 28; KTCL 140; UMCR 2 and 3; REC 14000; REC 15198; 768 ± VHL; RCC 4 ± VHL were originally obtained from the American Type Culture Collection (ATCC) and routinely cultured as recommended and as previously described (2-4). Human dermal microvascular endothelial cells were obtained from PromoCell (http://www.promocell.com/), cultured as recommended and as described in details elsewhere (1). All cell lines and primary cells were used at passage 4-10 and within 6 months after receipt for obtaining total RNA or protein. All cell lines and primary cells have been routinely tested and authenticated by the provider (ATCC). In addition, microvascular endothelial cells were characterized for their expression of endothelial cell-specific markers, e.g. CD31 etc. by immunofluorescence and flow cytometry analysis.

## SDS–PAGE and Immunoblotting

Protein lysates from cell lines and tissues were obtained and subjected to SDS–PAGE and immunoblotting as previously described (1).

**The Cancer Profiling Microarray Hybridization and Northern blotting**

The Cancer Profiling Microarray 7841 (cDNA microarray), consisting of normalized paired cDNA samples (n=241) generated from the total RNA from 13 organs (breast, uterus, colon, stomach, ovary, lung, kidney, rectum, thyroid, prostate, cervix, small intestine and pancreas), was obtained from Clontech (http://www.clontech.com). Each pair consisted of carcinoma and corresponding normal tissue samples obtained from the same patient. Paired cDNA represented the entire mRNA message expressed in given tissues. The microarray was used to provide comprehensive *ADM* gene-disease correlation data.

*ADM* cDNA was cloned into TOPO vector (Promega). *Ubiquitin* cDNA probe was from BD Biosciences. All vectors were sequenced using an Applied Biosystems 377 Genetic analyser, and sequences were checked against the GenBank database. Inserts were excised with restriction enzymes and labeled with $^{32}$P-dCTP using MegaPrime labeling Kit (GE Healthcare). The specificity of the probes was confirmed by Northern blotting, which was performed as previously described (5). Cancer Profiling Microarray was consequentially hybridized with each individual probe according to the manufacturer's instructions. For each probe, after hybridization and stringent washes, the microarray and blot were exposed to Hyperfilm (GE Healthcare) and subsequently to Phosphoscreen. The probe was then stripped and the hybridization with next probe performed. The hybridization signals were further analyzed using ImageQuant software. Ratio *ADM*/*Ubiquitin* was calculated to determine the relative mRNA expression levels and scatter plot graphs were generated using GraphPrism software.

**RNA Isolation, cDNA Synthesis, Quantitative Real-Time Quantitative Polymerase Chain Reaction (qRT-PCR) and Reverse Transcriptase PCR (RT-PCR)** were performed as previously described (5, 6). In brief, qRT-PCR reactions were performed in triplicate using the Corbett Research

Rotor Gene RG-3000 (now Qiagen; Sydney, Australia). Each reaction was performed in an individual tube and made up to 25 µl containing the equivalent of 5 ng of reverse transcribed RNA, 12.5 µl TaqMan 2X PCR Master Mix (Applied Biosystems, Foster City, CA) and 1.25 µl of the probe/primer mix. Conditions for the PCR reaction were 2 min at 50°C, 10 min at 95°C and then 40 cycles, each consisting of 15 s at 95°C, and 1 min at 60°C. The following primer/probe kits were used: Hs00181605_m1 (*ADM*) and Hs99999903_m1 (β-actin; *ACTB*) (both from Applied Biosystems). Human *ACTB* was used as reference gene to normalize for differences in the amount of total RNA in each sample. The reaction efficiency for each gene was calculated after obtaining standard curves for each PCR reaction by making two-fold serial dilutions covering the range equivalent to 20–0.625ng of RNA. Relative quantification of gene expression was performed using previously described method (7). In brief, comparisons were made between the number of cycles required for the fluorescence of a sample to reach a pre-determined threshold that lay within the exponential phase and above non-specific background. The relative ratio of gene expression was calculated as follows:

$$\text{Relative Ratio} = \frac{(E_{target})\,\Delta^{\text{Ct TARGET( mean comparator – mean sample)}}}{(E_{ref})\,\Delta^{\text{Ct REF (mean comparator-mean sample)}}}$$

$E_{target}$ = reaction efficiency of the gene of interest, $E_{ref}$ = reaction efficiency of the reference gene, $\Delta$Ct = the cycle difference between the comparator and the sample. All calculations are based on the mean value of PCR reactions performed in triplicate. The comparator for the clinical samples was the median normal kidney.

RT-PCR for *ADM*, β-actin (*ACTB*) and receptor activity modifying proteins (*RAMPs 1, 2* and *3)* mRNAs was performed using previously described sets of primers (5).

## Supplementary Figure Legends

**Supplementary Figure S1. Transcriptional profile of *ADM* expression in paired patient-matched normal and carcinoma tissues.** *ADM* gene expression was analyzed using the Cancer Profiling cDNA Array (Clonetics), which consists of normalized paired normal and cancer cDNA samples (n=241 pairs) generated from the total RNA from 13 organs (1- breast; 2-uterus; 3-colon; 4-stomach; 5-ovary; 6-lung; 7-kidney; 8-rectum; 9-thyroid; 10-prostate; 11-cervix; 12-small intestine; 13-pancreas) (see Figure 1B in the main text). The array was used to provide comprehensive *ADM* gene-disease correlation data. For details of hybridization please refer to the Materials and Methods in the main text and in the Supplemental Data. The array was exposed to Phosphoscreen and hybridization signals were analyzed using ImageQuant software. Ratio *ADM*/*ubiquitin* was calculated to determine the relative *ADM* mRNA expression levels (*Relative quantity of ADM mRNA*) and to generate jittered dot-plot graphs for each cancer type (numbered 1 to 10, corresponding to the cDNA array image on Figure 1B in the main text). Quantitative data for cancers 11, 12 and 13 is not presented due to small number of paired normal and cancer samples on the cDNA array. Statistical analysis was performed using Wilcoxon signed rank test and actual P values are indicated. For the reference to individual subtypes of cancers (i.e. breast, uterus, colon etc.) please see Cancer Profiling Array I Manual (cDNA array 7841; BD Biosciences; http://www.clontech.com).

**Supplementary Figure S2. CLR expression in tumor cells and tumor vessels in renal carcinoma.** The renal cancer profiling TMA included paired carcinoma and corresponding normal tissue samples from individual patients (n=87; including 69 RCC cases) as described in the Materials and Methods and Table 1. CLR localization (*CLR*; *left image*) was assessed by immunohistochemistry using anti-CLR antibody LN1436 (1). Secondary goat anti-rabbit antibody conjugated to horseradish peroxidase

was used and further detected with DAB (*brown color*). Cell nuclei were counter-stained with haematoxylin (*blue color*). Immunostaining with pre-immune serum from the same rabbit, in which the antibody was raised, was used as a control (*IgG control; right image*). **A,** CLR localization in histologically different types of renal tumors is shown at low magnification (*left column of images*) and at high magnification (*central column of images*). Note that the receptor is localized predominantly in the vessels (*arrows*) in glomeruli and between tubules in normal tissue (upper row of images) and in carcinomas (*RCC* – clear cell and *PRCC* – papillary carcinomas and *TCC* – transitional cell carcinoma of the renal pelvis) as well as oncocytoma and sarcomatoid renal cancers; and also in normal epithelial cells and in renal neoplastic cells (both - *arrowheads*). **B,** CLR expression levels in tumor cells in RCC vary, as shown in presented here six cases (*RCC-1 to RCC-6*). Note that the quantification data comparing CLR-immunoreactivity in paired RCC and corresponding normal tissue samples from the same patients (n=69 pairs) and CLR protein-disease correlation data (n=69 RCC cases) are presented in Figure 3A in the main text.

**Supplementary Figure S3. High CLR expression in tumor cells and tumor vessels in renal cancers compared to normal tissues and its association with histology.** The semi-quantitative analysis of the TMA data for CLR immunostaining (Figure 2 in the main text) was performed as described in the Materials and Methods and used to provide comprehensive CLR protein-disease outcome correlation data as shown on bar graphs (mean ± S.D.). **A,** CLR expression in renal cancers (all cancer types were taken into account when analyzing samples, n=87 paired patient-matched tumor and corresponding control/normal tissue samples). **B,** CLR expression in tumor cells and tumor vessels in RCC or various other histological types was compared to that in normal epithelial cells or vessels in patient-matched control normal kidney tissue (*N*). CLR expression was analyzed in clear cell renal cell carcinomas (*RCC*; n=69 patient-matched paired cancer and corresponding normal tissue samples), and

in more rare types of renal cancers, including papillary (*PRCC*), sarcomatoid, oncocytoma or transitional cell carcinomas (*TCC*; 6 unmatched tumor samples). Samples were paired where possible. **A-B,** Statistical analysis was performed using paired *t* test. Actual P values and numbers of analysed pairs of patient-matched tissue samples are shown.

**Supplementary Figure S4. Terminal glycosylation of CLR expressed in renal tumor tissues and cell lines. A,** Immunoblotting analysis of CLR expression in normal (*N*) and carcinoma (*C*) renal tissues was performed using protein lysates (20 μg) from patient-matched (*P1-6; P1-4 – RCC; P5 – benign; P6 - oncocytoma*) samples. CLR is terminally glycosylated (*black diamond*) and not core-glycosylated (*white diamond; (8-10)*). Note that in some cases total CLR is up-regulated in renal cancers (*P1, 2 and 4),* when compared to normal tissues, but in others it is down-regulated (*P3, 5 and 6*). **B,** Immunoblotting analysis of CLR expression in renal tumor cell lines. Terminally glycosylated CLR is endogenously expressed in some (designated *"CLR-high/positive"*), but is absent in other (designated *"CLR-low/negative"*) tumor cell lines, as detected by immunoblotting. Note that *in vitro*, endogenous CLR expression in cultured microvascular endothelial cells is higher, when compared to tumor cells; in accordance to its differential expression in microvascular endothelium and neoplastic cells *in vivo* (Figure 2 in the main text and Supplementary Figure S2). *Asterisk* indicates lower MW band detected by the antibody LN1436 in some renal tumor cell lines and in some tissues. **A-B,** Beta-actin (ACTB) served as a loading control.

**Supplementary Figure S5. Expression of *ADM* and *RAMPs* 1, 2 and 3 mRNAs in cell lines and renal tissues** was analyzed by reverse transcriptase PCR (RT-PCR). RNA samples were from renal tumor cell lines *KTCL 140*, *Caki-1* and *SKRC 28*, from human microvascular endothelial cells (*MVEC*) and from three patient-matched (*P1-3*) normal (*N*) and carcinoma (*C*) renal tissues. The set of primers

for the detection of human β-actin (*ACTB*) was used for loading controls, and DNA markers (*Ladder*) was used to confirm the size of the amplified PCR fragments.

**Supplementary Figure S6. High CLR expression in tumor cells and tumor vessels in renal tumors compared to normal tissues and its association with T stage.** The semi-quantitative analysis of the TMA data for CLR immunostaining (Figure 2 in the main text) was performed as described in the Materials and Methods and used to provide comprehensive CLR protein-disease outcome correlation data as shown on bar graphs (mean ± S.D.). CLR expression in tumor cells and tumor vessels in renal tumors of various T stages (according to TNM classification) was compared to that in normal epithelial cells or vessels in patient-matched normal control kidney tissues. Statistical analysis was performed using paired *t* test. Actual P values are shown; n – number of analysed pairs of patient-matched tissue samples.

## Supplementary References

1. Nikitenko LL, Blucher N, Fox SB, Bicknell R, Smith DM, Rees MC. Adrenomedullin and CGRP interact with endogenous calcitonin-receptor-like receptor in endothelial cells and induce its desensitisation by different mechanisms. J Cell Sci. 2006;119:910-22.

2. Okuda H, Toyota M, Ishida W, Furihata M, Tsuchiya M, Kamada M, et al. Epigenetic inactivation of the candidate tumor suppressor gene HOXB13 in human renal cell carcinoma. Oncogene. 2006;25:1733-42.

3. Wykoff CC, Pugh CW, Maxwell PH, Harris AL, Ratcliffe PJ. Identification of novel hypoxia dependent and independent target genes of the von Hippel-Lindau (VHL) tumour suppressor by mRNA differential expression profiling. Oncogene. 2000;19:6297-305.

4. Adam PJ, Terrett JA, Steers G, Stockwin L, Loader JA, Fletcher GC, et al. CD70 (TNFSF7) is expressed at high prevalence in renal cell carcinomas and is rapidly internalised on antibody binding. Br J Cancer. 2006;95:298-306.

5. Nikitenko LL, Brown NS, Smith DM, MacKenzie IZ, Bicknell R, Rees MC. Differential and cell-specific expression of calcitonin receptor-like receptor and receptor activity modifying proteins in the human uterus. Mol Hum Reprod. 2001;7:655-64.

6. Patel NS, Li JL, Generali D, Poulsom R, Cranston DW, Harris AL. Up-regulation of delta-like 4 ligand in human tumor vasculature and the role of basal expression in endothelial cell function. Cancer research. 2005;65:8690-7.

7. Pfaffl MW. A new mathematical model for relative quantification in real-time RT-PCR. Nucleic Acids Res. 2001;29:e45.

8. McLatchie LM, Fraser NJ, Main MJ, Wise A, Brown J, Thompson N, et al. RAMPs regulate the transport and ligand specificity of the calcitonin-receptor-like receptor. Nature. 1998;393:333-9.

9. Nikitenko LL, Cross T, Campo L, Turley H, Leek R, Manek S, et al. Expression of terminally glycosylated calcitonin receptor-like receptor in uterine leiomyoma: endothelial phenotype and association with microvascular density. Clin Cancer Res. 2006;12:5648-58.

10. Hilairet S, Foord SM, Marshall FH, Bouvier M. Protein-protein interaction and not glycosylation determines the binding selectivity of heterodimers between the calcitonin receptor-like receptor and the receptor activity-modifying proteins. J Biol Chem. 2001;276:29575-81.

# Supplementary Figure S1

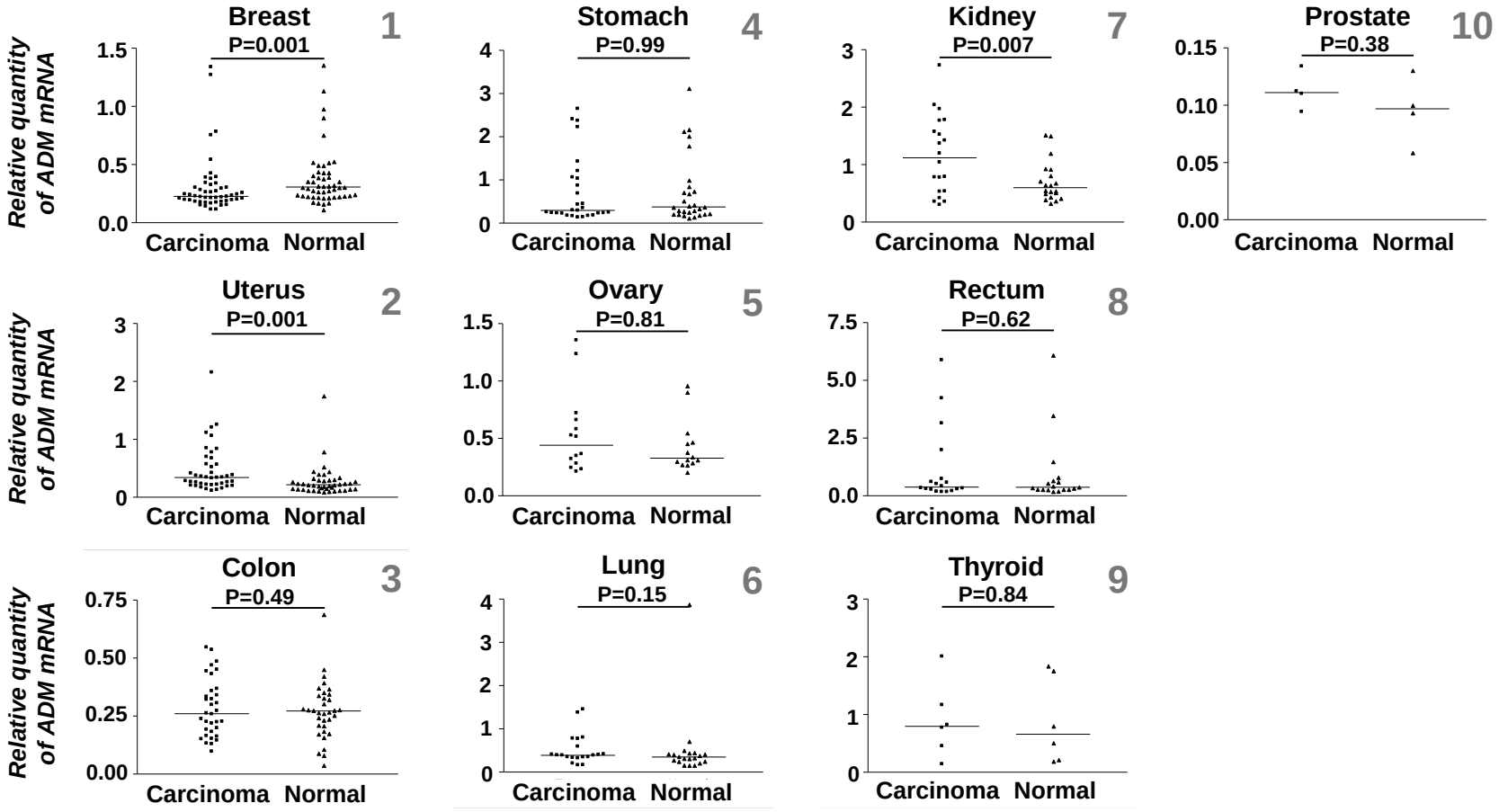

# Supplementary Figure S2

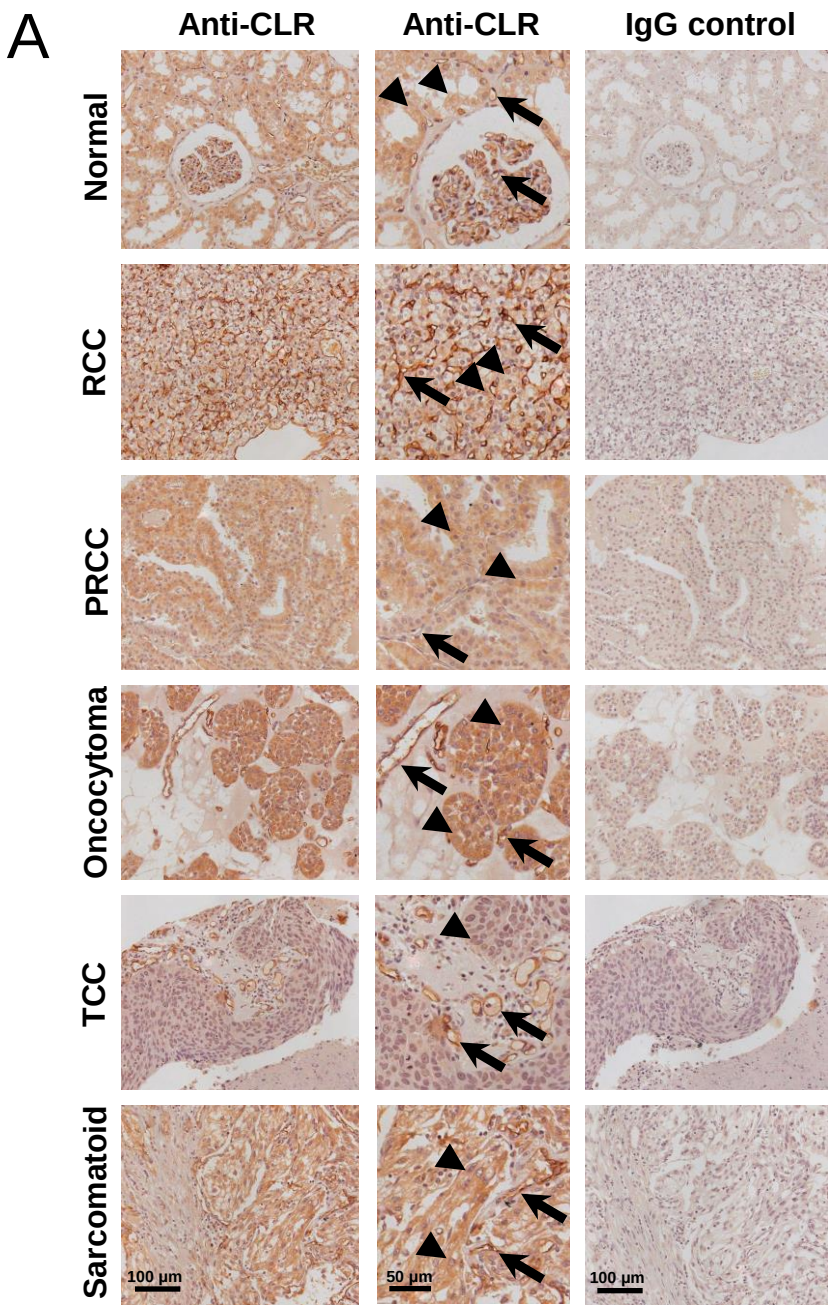

# Supplementary Figure S2

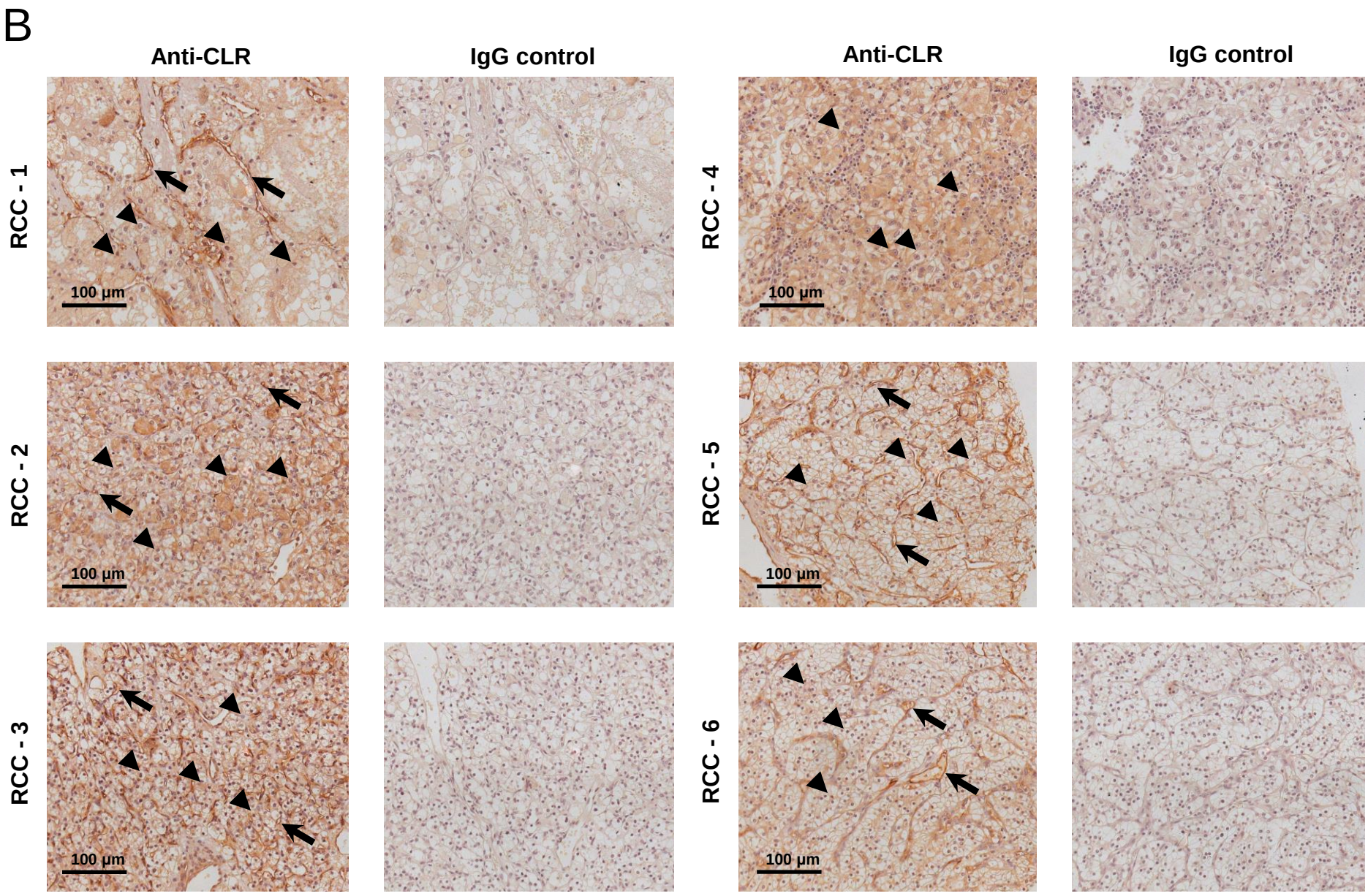

# Supplementary Figure S3

A

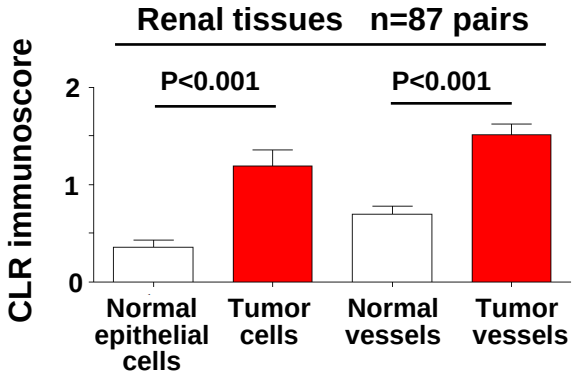


B

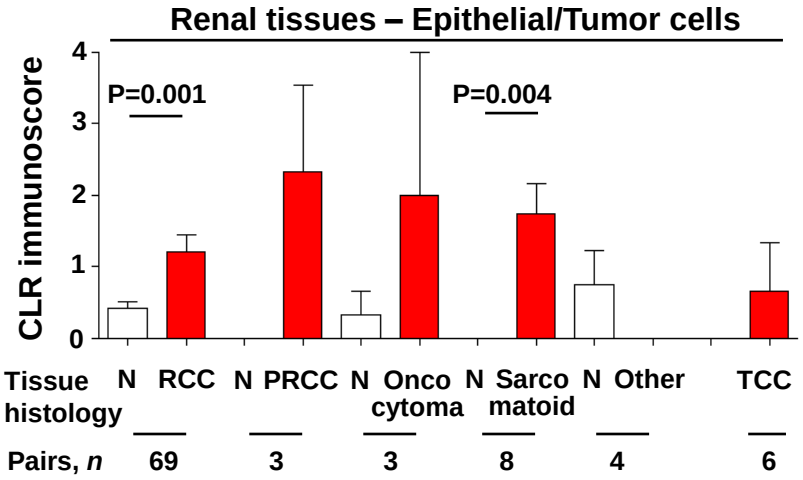


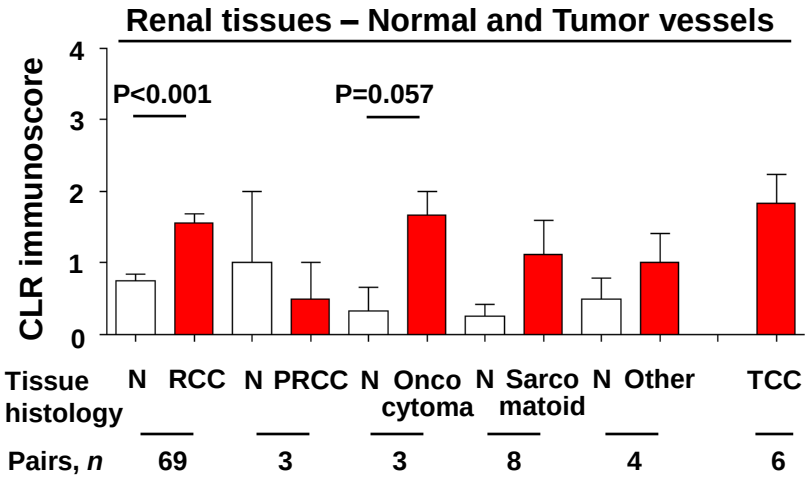

# Supplementary Figure S4

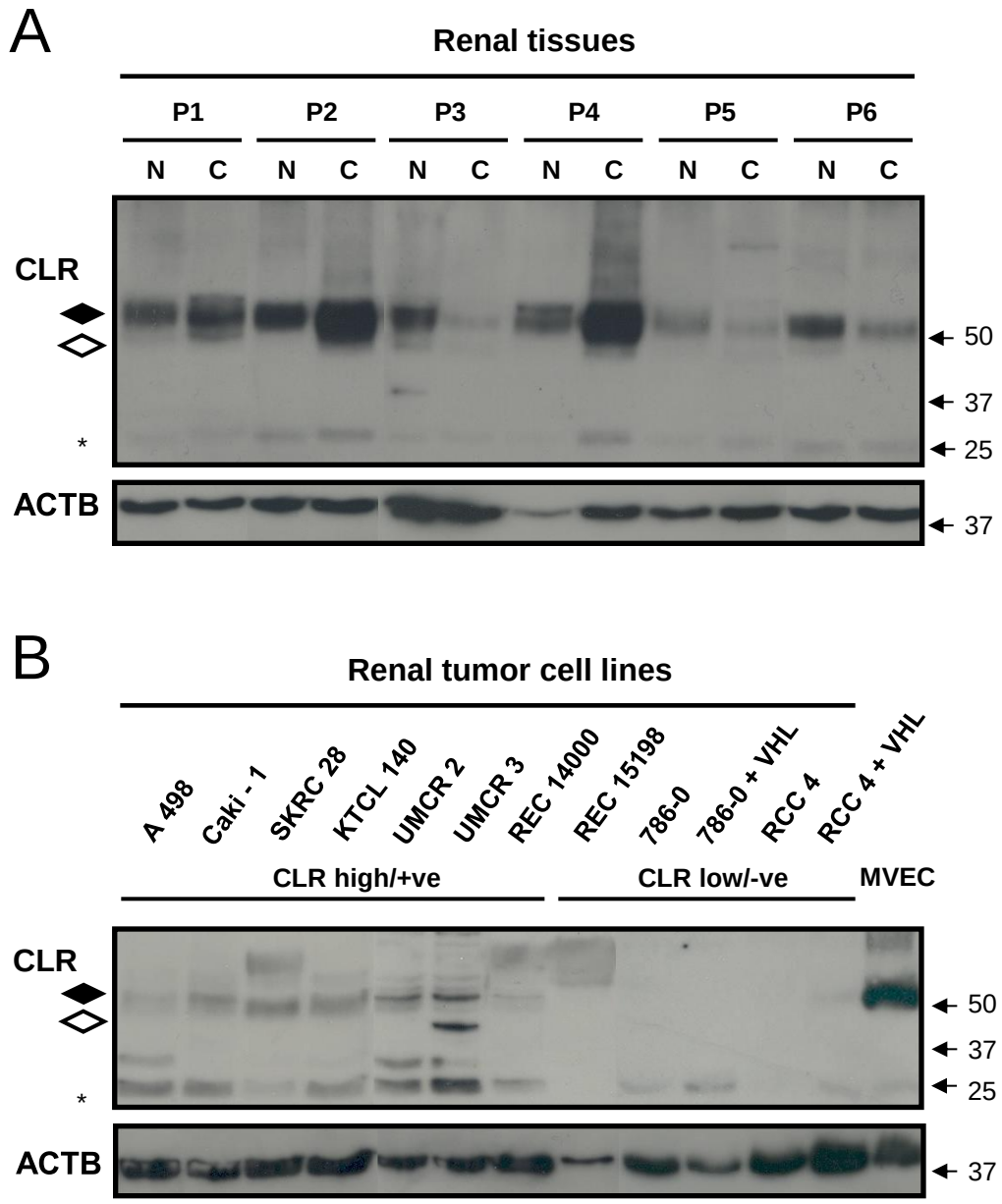

# Supplementary Figure S5

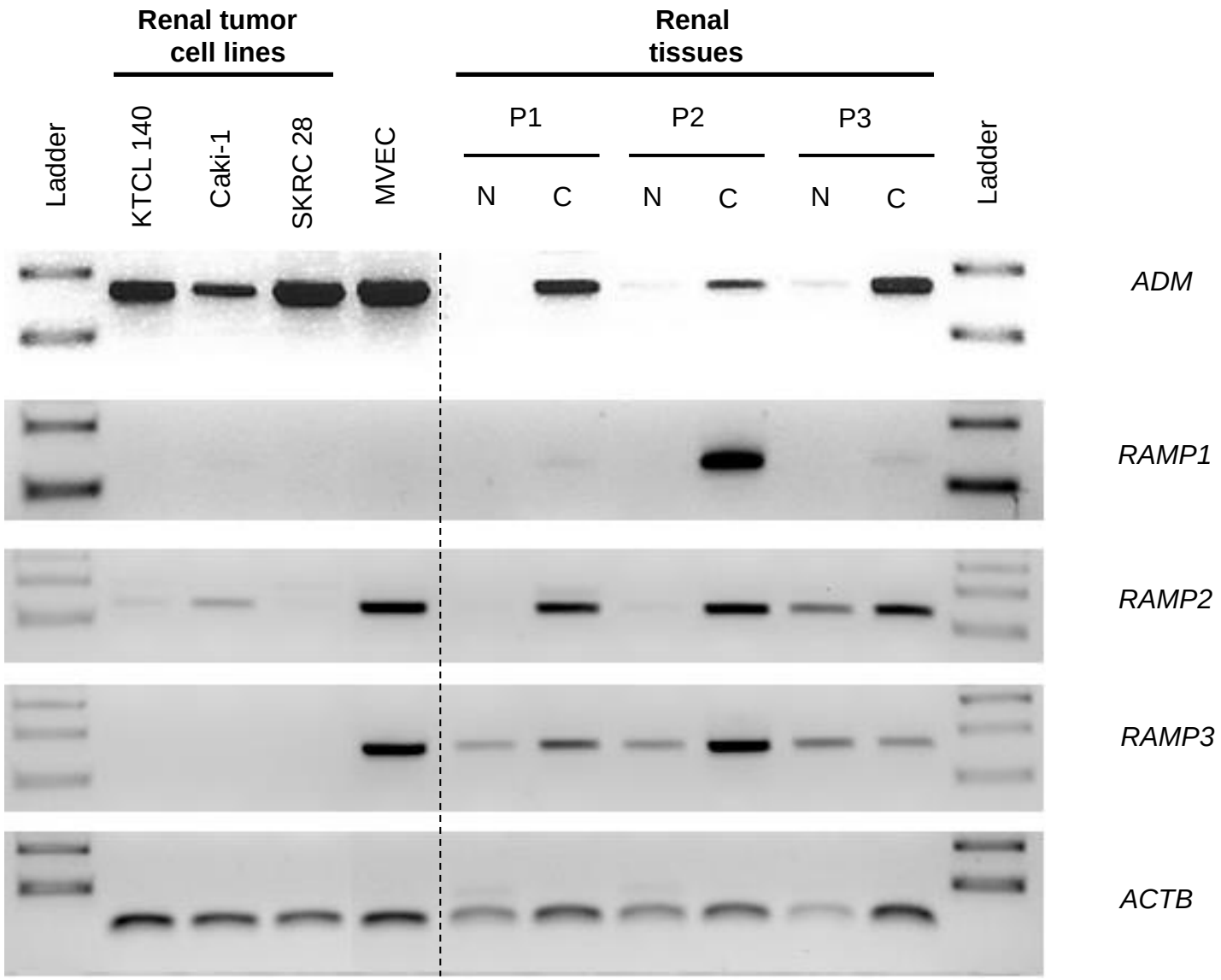

# Supplementary Figure S6